Dynamical Mean Field Theory of an Effective Three-Band Model for Na_xCoO_2

A. Bourgeois,[1] A. A. Aligia,[2] and M. J. Rozenberg[1]

[1]*Laboratoire de Physique des Solides, Université Paris-Sud, CNRS UMR-8502, 91405 Orsay cedex, France*

[2]*Centro Atómico Bariloche and Instituto Balseiro, Comisión Nacional de Energía Atómica, 8400 Bariloche, Argentina*

(Received 22 October 2008; published 12 February 2009)

We derive an effective Hamiltonian for highly correlated t_{2g} states centered at the Co sites of Na_xCoO_2. The essential ingredients of the model are an O mediated hopping, a trigonal crystal-field splitting, and on-site effective interactions derived from the exact solution of a multiorbital model in a CoO_6 cluster, with parameters determined previously. The effective model is solved by dynamical mean field theory. We obtain a Fermi surface and electronic dispersion that agrees well with angle-resolved photoemission spectra. Our results also elucidate the origin of the ''sinking pockets'' in different doping regimes.

DOI: 10.1103/PhysRevLett.102.066402 PACS numbers: 71.27.+a, 71.18.+y, 74.25.Jb, 74.70.−b

The construction of the appropriate low-energy Hamiltonian to describe a highly correlated system is a crucial task for an advance in its physical understanding. A clear example is the case of the superconducting cuprates. The starting point for the description of those materials is a three-band model containing the most relevant Cu and O orbitals. The parameters of that model were determined by constrained-density-functional theory [1]. On the basis of the exact solution of the multiband model in a CuO_4 cluster (containing one Cu atom and its four nearest neighbors), Zhang and Rice suggested that the essential low-energy physics of the model is captured by a one-band model containing only effective Cu orbitals [2]. This has been confirmed by systematic derivations of the ensuing one-band Hubbard and t-J models [3,4]. These models have led to considerable progress in the understanding of the high-T_c cuprates. Similar low-energy effective models were derived and used successfully to explain the properties of nickelates [5,6] and other transition metal oxides [7].

In the cobaltates Na_xCoO_2 a consensus has not yet been reached on the appropriate low-energy effective Hamiltonian, as different approaches have provided conflicting results. The cobaltates present a clear-cut example of strong correlation effects, not only by its rich phase diagram that includes a charge ordered insulator and a superconducting state, but also by the complete failure of the *ab initio* band-structure calculations to describe the shape of the Fermi surface (FS) measured in angle-resolved photoemission spectra (ARPES) experiments [8,9]. First-principles calculations done in the local-density approximation (LDA) [10] predicted a FS with six prominent hole pockets along the Γ-K direction, which were never detected in photoemission. In addition, the ARPES experiments have revealed the presence of dispersive features at the momenta positions where those pockets were expected, but they were observed at about 0.2 eV beneath the FS. Thus, they were termed ''sinking pockets'' and are still awaiting a clear physical interpretation.

Initial theoretical progress was seemingly achieved by Zhou *et al.* [11] who included correlation effects on top of a tight-binding model fit to the band structure from first-principles calculations in the LDA [10]. They showed that correlation effects may in fact wipe out the pockets by reducing the bandwidth of the bands crossing the Fermi energy. However, the approach of Zhou *et al.* relied on a simplified static Gutzwiller approximation where the rather unrealistic assumption of an infinite strength for the local effective t_{2g} Coulomb repulsion U is made. In a different approach to the problem, Ishida *et al.* [12] used the more elaborate dynamical mean field theory (DMFT) methodology to treat the correlation effects, on top of a similar LDA-derived tight-binding Hamiltonian. The main finding of that work was the prediction that the effect of finite U is, in marked contrast to the Gutzwiller approximation, to actually *increase* the size of the LDA pockets that get stabilized by $e'_g - a_{1g}$ charge transfer.

Marianetti *et al.* [13], using a DMFT calculation similar to Ishida *et al.*, found that the pockets can be made to disappear for sufficiently large values of U (above 6 eV), which explained their absence in the infinite U calculation. Although for realistic values of U the pockets still remained, those authors also pointed out that using the $e'_g - a_{1g}$ crystal-field splitting as a free fitting parameter they could eventually be made to disappear. More recently, Liebsch and Ishida [14] critically discussed the various previous approaches that were based on the LDA band structure as the starting point for the calculation of correlation effects. They concluded that, at values $U \sim 3$ eV which they considered realistic, the presence of pockets in the Fermi surface is always predicted. They argued that this feature, which is in conflict with ARPES data, is robust with respect to the details of the LDA fits and to the form of the interaction term.

A simple-minded identification of the LDA conduction bands as the relevant manifold where correlations are to be included (as in LDA + DMFT) may not be fully justified when systems have a strong covalent character, as is the case of the cobaltates. In particular, it was shown that the above procedure fails in NiO, and agreement with experiments in LDA + DMFT calculations is only achieved once

the O bands are explicitly included in the model [15]. Interestingly, the results of that approach also agree with results from effective models where the O atoms have been integrated out using low-energy reduction procedures that take into account correlations from the beginning [5,15].

We propose to address the problem of the low-energy description of the band structure of the cobaltates by taking a different approach and altogether leave the LDA as the starting point of our calculation. Thus, in this Letter we perform a low-energy reduction to derive an effective Hamiltonian $H_{\rm eff}$ that includes the determination of effective local interactions, and then study its physical behavior using DMFT. The derivation of $H_{\rm eff}$ follows the ideas of previous research in the cuprates which used the cell-perturbation method [3] and nonorthogonal Zhang-Rice singlets [2,4] constructions. Basically, the procedure is to divide the system in different cells that are solved exactly, and retain their lowest energy states. Then, one includes the intercell terms along with the effect of the other states as perturbations to this low-energy subspace. The resulting effective Hamiltonian differs substantially from those previously adopted. In particular, our calculated value of U is significantly smaller, again raising questions on the justification of the assumption of an infinite value for the Coulomb interaction made in Gutzwiller-type approaches. This observation also applies to a recent Gutzwiller density-functional calculation that reports good agreement with ARPES data, in which $U \gtrsim 3$–5 eV was assumed [16].

We start from the exact solution of a CoO_6 cluster model containing all $3d$ orbitals of a Co atom and all $2p$ orbitals of its six nearest-neighbor O atoms, assuming cubic (O_h) symmetry and neglecting spin-orbit coupling. All interactions inside the $3d$ shell are included [17]. The parameters were determined fitting x-ray-absorption spectroscopy experiments and its polarization dependence [17]. The results show a large Co-O covalency and an intraorbital repulsion $U_m = 4.5$ eV, larger than the Co-O charge-transfer energy. The subscript m refers to the original multiband model, to distinguish U_m from the corresponding repulsion U of the effective model, which, as shown below, is strongly reduced due to Co-O covalency. We recall that in the cuprates, $U_m \sim 10$ eV [1], while in their effective low-energy one-band Hubbard model $U \sim 3$ eV [3].

The effective model $H_{\rm eff}$ is obtained mapping the ground state of the CoO_6 cluster with four holes onto the on-site vacuum of $H_{\rm eff}$ (no t_{2g} holes at a Co site, i.e., Co^{3+}), and the sixfold degenerate (spin doublet and orbital triplet) ground state for five holes onto the corresponding states with one t_{2g} hole of $H_{\rm eff}$. Details of the mapping are given in Ref. [18]. We remark that Co^{3+} and Co^{4+} in $H_{\rm eff}$ actually represent highly correlated states with a Co valence near 2.04 and 2.56, respectively [17]. The ''noninteracting'' part of $H_{\rm eff} = H_0 + H_I$ can be written as

$$H_0 = \sum_{i,j} \sum_{\alpha,\alpha',\sigma} (t^{ij}_{\alpha\alpha'} + t'^{ij}_{\alpha} \delta_{\alpha\alpha'} + D_{\alpha\alpha'} \delta_{ij}) d^\dagger_{i\alpha\sigma} d_{j\alpha'\sigma}, \quad (1)$$

where $d^\dagger_{i\alpha\sigma}$ creates a hole in the t_{2g} orbital α (xy, yz, or zx) with spin σ at site i. However, physically this operator represents a nontrivial excitation of the same symmetry, which also involves $3d$ e_g orbitals of Co and $2p$ orbitals of nearest-neighbor O sites. t' and t correspond to the direct Co-Co hopping and to that mediated by O $2p_\pi$ orbitals, respectively. The latter is the most important one and has been calculated before using many-body eigenstates of the CoO_6 cluster [18]. Finally, D accounts for the trigonal crystal-field splitting $\Delta = 3D$ between e'_g and a_{1g} orbitals. We take it from quantum-chemistry configuration-interaction calculations [19]. These are the most reliable methods to determine crystal-field excitations. Incidentally, it is known that while the LDA may provide a good description of the ground-state, it does not get the energy of excited states right. Therefore it is not expected to provide accurate values for D in a highly correlated system. Note that although H_0 has the form of a noninteracting Hamiltonian, the derivation of its parameters already involves many-body calculations [18,19]. In fact, similarly as in the studies of cuprates, most of the original Co on-site interaction is already included in the derivation of $H_{\rm eff}$ through the diagonalization of the CoO_6 cluster.

The interacting part of $H_{\rm eff}$ is

$$H_I^i = \sum_i H_I^i;$$

$$H_I^i = U \sum_\alpha n_{i\alpha\uparrow} n_{i\alpha\downarrow} + \frac{1}{2} \sum_{\alpha\neq\beta,\sigma\sigma'} (U' n_{i\alpha\sigma} n_{i\beta\sigma'} + J d^\dagger_{i\alpha\sigma} d^\dagger_{i\beta\sigma'} d_{i\alpha\sigma'} d_{i\beta\sigma}) + J' \sum_{\alpha\neq\beta} d^\dagger_{i\alpha\uparrow} d^\dagger_{i\alpha\downarrow} d_{i\beta\downarrow} d_{i\beta\uparrow}, \quad (2)$$

where the interaction parameters were calculated from the comparison between the energy of adding two holes in the same CoO_6 cluster with given symmetry and spin, or in different clusters. The eigenvalues of H_I^i with two holes should coincide with the corresponding lowest energy levels for six holes in the cluster. The resulting parameters of the model become $t = 0.10$ eV, $D = 0.105$ eV, $U = 1.86$ eV, $U' = 1.27$ eV, $J = 0.35$ eV, and $J' = 0.17$ eV. To our knowledge, this the first time that a calculation of the interaction terms is reported in this system. Note that the values of the U parameters are smaller than those used in previous calculations [11–13], but are still much larger than the bandwidth. We took $t' = 0.02$ eV, which provides the best agreement with experiment; however, our main results are not affected by the specific chosen value.

Here we solve $H_{\rm eff}$ using the DMFT [20]. The associated quantum impurity problem is a three-orbital Anderson impurity that is solved using the Hirsch-Fye quantum Monte Carlo (QMC) algorithm [21]. Because of the symmetry of the band structure of H_0, the DMFT quantum impurity problem, its corresponding self-consistency constraint (Dyson equation), and local self-energies $\Sigma^{\rm DMFT}_{\alpha,\sigma}$ are diagonal in orbital and spin indexes. In order to obtain the

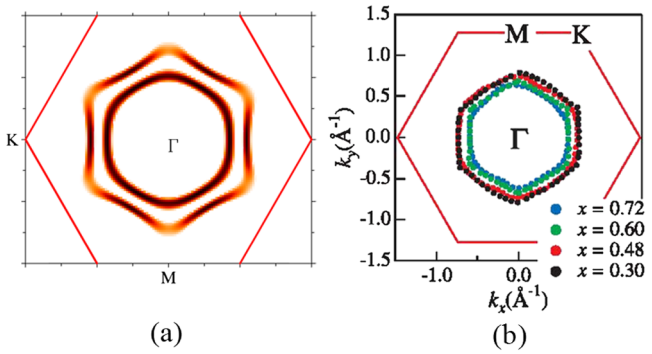

FIG. 1 (color online). (a) Calculated FS for dopings $x = 0.3$ and $x = 0.7$ [inner (hole) edge of larger and smaller hexagon, respectively]. (b) ARPES measurements from [8].

momentum and energy resolved Green's functions, the local self-energies have to be analytically continued to the real frequency domain. Thus, we obtained high quality QMC data using over 10^6 sweeps to reliably perform the continuation by means of a standard maximum entropy method [22]. In the calculations presented here, J' and the spin flip terms in Eq. (2) were neglected. This simplification introduces tiny modifications in the results [14]. Thus, we adopt the interaction parameters $U_{\alpha,\alpha} = U = 1.86$ eV for the intraorbital repulsion, and $U^{\sigma,-\sigma}_{\alpha,\alpha'} = U' = 1.27$ eV and $U^{\sigma,\sigma}_{\alpha,\alpha'} = U' - J = 0.92$ eV for the interorbital repulsions with opposite or the same spin, respectively.

The predicted band structure is then obtained from the imaginary part of the lattice Green's functions given by $G_\alpha(\mathbf{k}, \omega) = [\omega - \epsilon_{\mathbf{k},\alpha} - \Sigma^{\mathrm{DMFT}}_\alpha(\omega)]^{-1}$, and the Fermi surface is mapped out from the $\omega = 0$ crossings of the interacting bands.

For reasons of space, the data displayed in the figures are for doping $x = 0.3$ and 0.7, ranging from stronger to weaker correlations. Because of their high computational cost, the lowest temperature that we study is $T = 360$ K. Comparison with calculations at higher temperatures ($\sim$720 K) indicates that we have indeed achieved the low T limit. In addition, as will be shown later, the width of the quasiparticle band at the Fermi energy, which is the smallest energy scale in the electronic structure, is much larger than the temperature of the calculation.

In Fig. 1 we show our results for the evolution of the FS as a function of increasing doping along with the respective experimental ARPES data. We observe good agreement in the shape and size of the FS. Significantly, the hole pockets are absent in our results. The experimental FS for $x = 0.3$ is somewhat more rounded than the theoretical one. This may partially be due to the relatively large thermal broadening in the calculation, but may also be due to lack of hopping terms at longer distances, beyond those included in H_0.

The details of the band structure are shown in Fig. 2. We observe that the data reveal several contributions that can be associated with either coherent (i.e., quasiparticlelike) or incoherent (i.e., Hubbard) bands. The incoherent bands are characterized by dispersive structures similar to those of the "noninteracting" Hamiltonian H_0 (though usually less defined due to shorter lifetimes) that appear far from the Fermi energy. These large energy shifts are of course due to the local interactions of H_{eff} [Eq. (2)]. In the top left-hand panel of Fig. 2 we show the full band structure for the strongly correlated case $x = 0.3$. There, one can observe several incoherent bands that appear shifted down in energy, at ~ -1, -1.75, and -3 eV, with the first one carrying a large part of the spectral intensity. Their shapes reveal their dominant orbital content, and their energy shifts can be understood from the values of the interorbital and intraorbital Coulomb repulsions. At higher dopings, the correlation effects decrease and these incoherent bands rapidly lose spectral intensity. On the other hand, the

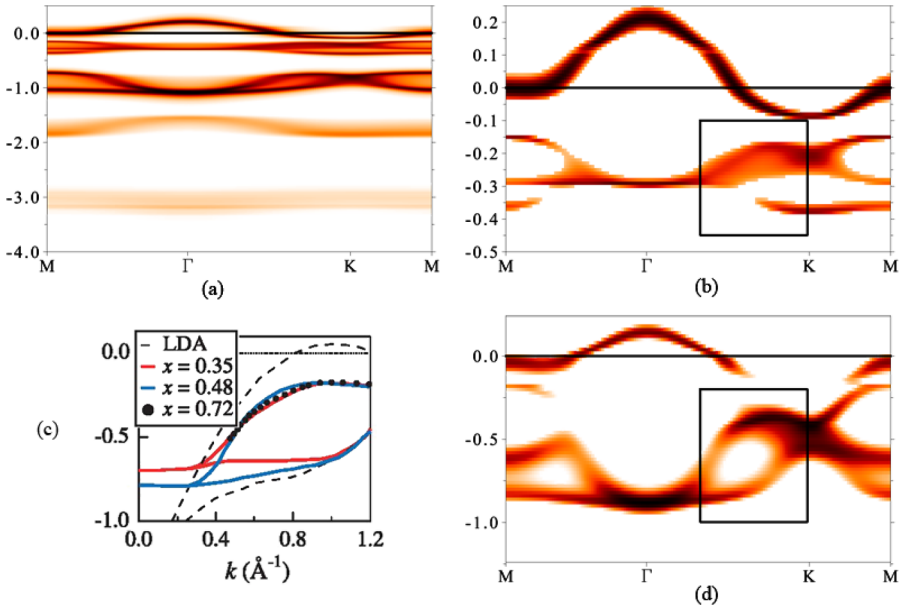

FIG. 2 (color online). (a) Full band structure for $x = 0.3$. The $x = 0.3$ and $x = 0.7$ cases are detailed in (b) and (d), respectively, where the structures in the dispersion corresponding to the sinking pockets are highlighted by a box. (c) Sinking pockets for various dopings, with comparison to LDA [8].

coherent bands are near the Fermi energy and their band structure is somewhat narrowed with respect to that of H_0 [Eq. (1)] due to the effect of H_I [Eq. (2)], indicating the enhancement of the effective mass.

The top right-hand panel of the figure shows details of the band structure at $x = 0.3$ and, for comparison with the less correlated case, the lower right-hand panel shows similar data for $x = 0.7$. Interestingly, these results reveal a novel insight on the nature of the ''sinking pockets,'' whose experimental data we reproduced in the lower left-hand panel. We find that while the sinking pockets are present at both low and high dopings (they are indicated by boxes in the respective panels), their physical origin is qualitatively different. At higher x, correlations are low and the band structure does not differ much from the noninteracting case. Thus, the sinking pocket in this case can be simply associated to the top of the band with mostly e'_g character. In contrast, at $x = 0.3$ (the strong correlation case), the band structure is dramatically modified and that interpretation is no longer possible. In fact, the strongest contribution to the e'_g band is shifted down in energy by about 1 eV. This shift is due to the interorbital Hubbard repulsion, and can be more easily understood in a hole picture. As there is about one hole in the a_{1g} band, putting a second hole costs $U_{a1g,e'g} \sim 0.92$–1.27 eV if the hole goes into the e'_g band [or $U_{a1g,a1g} \sim 1.86$ eV into the a_{1g} band [see Fig. 2(a)]. However, in the ground state there is also a non-negligible amplitude for a configuration with no holes in the a_{1g} band; thus, one may create a hole in the original e'_g band with no extra Coulomb energy cost. Such a state would have a reduced spectral intensity but a similar dispersion as that of the noninteracting e'_g band, thus accounting for the sinking pocket. This is confirmed by our calculations on the weight of the states with different symmetries in the coherent bands (not shown). A clear signature of this sinking pocket state is indicated by a box in our numerical data Fig. 2(b). We note that our results show a lower energy edge at ~ -0.2 eV in good agreement with all available ARPES data [8,9]. Nevertheless, the experimental situation is less clear for the determination of the dispersive shape of the sinking pockets at higher binding energies. With regard to the influence of possible Na ordering, recent ARPES experiments [9] conclude that that feature does not affect significantly the position of the sinking pockets in the unfolded Brillouin zone.

In conclusion, motivated by the apparent failure of LDA band structure to provide a sound starting point for the calculation of strong correlation effects in the cobaltates, we derive an effective low-energy Hamiltonian that includes the strength of the local Coulomb repulsive interactions. The effective model is obtained from finite cluster and quantum-chemistry calculations, with essentially no adjustable parameters. The effective Hamiltonian is treated with DMFT to compute the effects of correlations. We find that the evolution of the FS is in good agreement with the experimental data. Importantly, the LDA-predicted hole pockets, that are not seen in the ARPES data, are also not present in our results. One difference with respect to LDA calculations is how the effect of correlations separates the bands as discussed above. However, for realistic U this feature alone is not enough to destroy the pockets, and the value of D, usually underestimated by LDA, was also shown to play a key role. We obtained the detailed interacting electronic structure that reveals sinking pockets at all dopings. Significantly, their origin is qualitatively different in the high and low doping cases.

We thank V. Vildosola for help with the implementation of the QMC code, and V. Brouet for discussions on ARPES data. This investigation was sponsored by PIP 5254 of CONICET and PICT 2006/483 of the ANPCyT, and by the ECOS-Sud program. A. A. A. is partially supported by CONICET.

[1] M. S. Hybertsen *et al.*, Phys. Rev. B **41**, 11 068 (1990); J. B. Grant and A. K. McMahan, Phys. Rev. Lett. **66**, 488 (1991).
[2] F. C. Zhang and T. M. Rice, Phys. Rev. B **37**, 3759 (1988).
[3] L. F. Feiner, J. H. Jefferson, and R. Raimondi, Phys. Rev. B **53**, 8751 (1996); M. E. Simon, A. A. Aligia, and E. R. Gagliano, *ibid.* **56**, 5637 (1997), references therein.
[4] A. A. Aligia, M. E. Simon, and C. D. Batista, Phys. Rev. B **49**, 13 061 (1994).
[5] J. Bala, A. M. Oleś, and J. Zaanen, Phys. Rev. Lett. **72**, 2600 (1994).
[6] C. D. Batista, A. A. Aligia, and J. Eroles, Europhys. Lett. **43**, 71 (1998).
[7] P. Horsch *et al.*, Phys. Rev. Lett. **100**, 167205 (2008), and references therein.
[8] H. Yang *et al.*, Phys. Rev. Lett. **95**, 146401 (2005).
[9] D. Qian *et al.*, Phys. Rev. Lett. **97**, 186405 (2006).
[10] D. Singh, Phys. Rev. B **61**, 13 397 (2000); **68**, 020503(R) (2003); P. Zhang *et al.*, Phys. Rev. Lett. **93**, 236402 (2004); K. Lee, J. Kunes, and W. Pickett, Phys. Rev. B **70**, 045104 (2004).
[11] S. Zhou *et al.*, Phys. Rev. Lett. **94**, 206401 (2005).
[12] H. Ishida, M. Johannes, and A. Liebsch, Phys. Rev. Lett. **94**, 196401 (2005).
[13] C. Marianetti, K. Haule, and O. Parcollet, Phys. Rev. Lett. **99**, 246404 (2007).
[14] A. Liebsch and H. Ishida, Eur. Phys. J. B **61**, 405 (2008).
[15] J. Kunes *et al.*, Phys. Rev. Lett. **99**, 156404 (2007).
[16] G.-T. Wang, X. Dai, and Z. Fang, Phys. Rev. Lett. **101**, 066403 (2008).
[17] T. Kroll, A. A. Aligia, and G. Sawatzky, Phys. Rev. B **74**, 115124 (2006).
[18] A. Bourgeois *et al.*, Phys. Rev. B **75**, 174518 (2007).
[19] S. Landron and M. B. Lepetit, Phys. Rev. B **74**, 184507 (2006); **77**, 125106 (2008).
[20] A. Georges *et al.*, Rev. Mod. Phys. **68**, 13 (1996).
[21] M. J. Rozenberg, Phys. Rev. B **55**, R4855 (1997).
[22] J. Gubernatis *et al.*, Phys. Rev. B **44**, 6011 (1991); Phys. Rep. **269**, 133 (1996).